*International Journal of Engineering and Technology Innovation, vol. 7, no. 4, 2017, pp. 269 - 279*

# Thermal Analysis of a Cracked Half-Plane Under Moving Point Heat Source

Kuanfang He*, Qing Yang, Dongming Xiao, Xuejun Li

Hunan Provincial Key Laboratory of Health Maintenance for Mechanical Equipment, Hunan University of Science and Technology, Xiangtan, Hunan, China.

Received 24 October 2016; received in revised form 10 April 2017; accepted 12 April 2017

## Abstract

The heat conduction in half-plane with an insulated crack subjected to moving point heat source is investigated. The analytical solution and the numerical mean are combined to analyze the transient temperature distribution of a cracked half-plane under moving point heat source. The transient temperature distribution of the half plane structure under moving point heat source is obtained by the moving coordinate method firstly, then the heat conduction equation with thermal boundary of an insulated crack face is changed to singular integral equation by applying Fourier transforms and solved by the numerical method. The numerical examples of the temperature distribution on the cracked half-plane structure under moving point heat source are presented and discussed in detail.

**Keywords:** heat conduction, moving point heat source, insulated crack, the moving coordinate method, singular integral equation, numerical solution method

## 1. Introduction

There are many cases on thermal shock process study when a hot body is placed in contact with a cold one. Welding technique has been widely used in the modern industry and engineering fields such as the automobile and the computer components fabrication [1-2]. The mathematical model of the welding process could be simplified as a heat conduction process of a moving point heat source applied on a medium. Rosenthal [3] has derived analytical solution equations of a quasi-stationary thermal state for welding heat conduction. Christensen [4] also used an analytical-empirical approach and derived the dimensionless equations for heat flow during welding. The conventional analytical methods to solve heat conduction of welding are often complexand inapplicable in some cases. The interest about the numeric simulation problems of welding was gradually arousing, and the modeling of the heat transfer and fluid flow in the arc plasma for welding process has been well documented. Oreper [5] presented a mathematical formulation for the transient fluid-flow and the temperature field in the welding liquid pool. Choo [6] developed a mathematical formulation to describe the temperature profiles in gas tungsten arc welding (GTAW). Lowke [7] developed unified theory of arcs and electrodes that are used to make predictions of arc temperatures and voltages in argon. Recently, numerical analysis methods and computer programs for heat conduction and thermoelastic analysis have been commonly developed. Kou [8] used the numerical method for convection simulation. Kim [9] studied the heat and mass flow in moving arc welding pools by the numerical method. Fan [10] developed a two-dimensional axisymmetric numerical model to describe the heat transfer and fluid flow in the gas tungsten welding. Joshi [11] studied a three-dimensional computation to explain the rotational flow in aluminum welding pools. Tanaka [12] developed a numerical model to analyze the balances of mass, energy and force in the welding phenomena. Wei [13] proposed a three-dimensional finite element model to evaluate the dynamic thermal stress and strain contributed to the formation of solidification cracking. Hu [14] has developed a unified comprehensive model to simulate the transport phenomena during the gas metal arc welding process. Yaghi [15] has conducted finite element

* Corresponding author E-mail address: hkf791113@163.com

simulation of welding thermal and residual stresses in the specific heat of material. Das [16]developed a model of the heat transfer during welding by Element Free Galerkin(EFG) method, which demonstrated the effectiveness and utilities of the EFG method for modeling and understanding of the heat transfer processes in arc welding. Sheikhi [17] investigated the underlying mechanism of solidification crack in pulsed laser welding of 2024 aluminum alloy experimentally and numerically. The subjects of thermoelastic analysis in welding by the analytical solutions and numerical techniques mainly focus on the non-crack homogeneous or nonhomogeneous plane structure.

There are many available literatures and referenced results about heat conduction analysis for a cracked homogeneous or nonhomogeneous plane structure under thermal boundary conditions. Sih [18] conducted mathematical analysis of the heat flux and temperature in the neighborhood of a line of discontinuity in the infinite region by a uniform steady heat flow. Tzou [19] investigated the singular behavior of the temperature gradient and thermal behavior in the vicinity of discontinuities. Noda and Jin [20] solved the crack problems in nonhomogeneous thermoelastic solids of the Functionally Gradient Material under steady thermal loadings. Zhou et al [21] calculated and analyzed thermal response of an orthotropic functionally graded coating-substrate structure with a partially insulated interface crack under a steady-state heat flux supply. Jin and Noda [22] modeled a semi-infinite plate of a functionally gradient material with a crack under transient thermal loading conditions. Manson and Rosakis [23] investigated thermal stresses around a crack in thermo-elastic materials, and measured the temperature distribution at the tip of a dynamically propagating crack experimentally. Chang and Ma [24] computed transient thermal conduction of a rectangular plate with multiple insulated cracks by the alternating method. Zamani et al [25] investigated the effect of second sound of Lord–Shulman theory on a cracked layer under thermal shock. Wang and Han [26] introduced Non-Fourier heat conduction into thermoelastic fracture mechanics, and investigated the problem of a finite crack in a material layer subjected to a transient heat flow. Hu and Chen [27]analyzed the transient temperature and thermal stresses around a crack in thermoelastic materials using the hyperbolic heat conduction theory. Hu and Chen [28] also investigated the transient temperature field around a crack in half-plane under temperature impacts using the DPL heat conduction model.

The thermal distribution in the inherent finite-length crack subjected to the moving point heat source has not yet been reported in the above literatures. In recent years, the research of numerical solution in heat conduction has been further developed and applied in heat conduction fields [29-30]. In this paper, the thermal analysis of a cracked half-plane is studied under a moving point heat source by analytical solution and the numerical means. The moving coordinate method is adopted to change the heat conduction under transient moving point heat source into steady one, and obtain the analytical solution of the non-crack half plane structure. The heat conduction equation with thermal boundary of crack face is changed to be singular integral equation by applying Fourier transforms and solved by a numerical method. The temperature distribution of a cracked half-plane under moving point heat source are computed and analyzed by the analytical solution and the numerical means.

## 2. Basic Equation

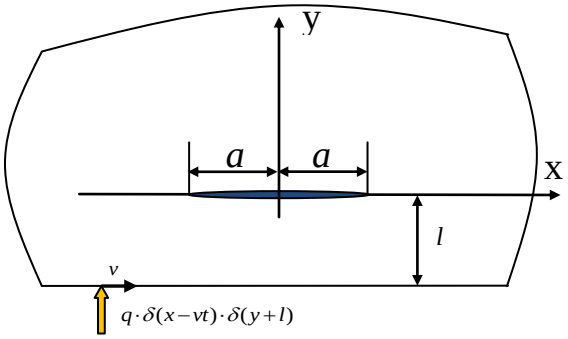


Fig. 1 Geometry and coordinates for a cracked semi-infinite plate under moving point heat source

A semi-infinite thermoelastic plate structure containing a through crack is shown in Fig. 1. The crack is parallel to the boundary of the structure with length of 2$a$. The Cartesian coordinate system is denoted by ($x$, $y$) with the origin at the middle point of the crack face along with the $x$ direction. A heat intensity $q$ of the point heat source is moving at the speed of $v$ in $x$-direction with the parallel distance of $l$ to the crack face in $y$-direction. The position of the heat intensity $q$ is ($vt$, -$l$). The Fourier's law of heat conduction is

$$k\nabla^2 T - \rho c\frac{\partial T}{\partial t} = -q.\delta(x - vt).\delta(y + l) \tag{1}$$

where $q$ is the heat intensity of the heat source, $T$ is the temperature, $k$ is the thermal conductivity of the material, $\rho$ and $c$ are the mass density and the specific heat capacity, $\nabla$ is the spatial gradient operator, $t$ is the physical time, and $v$ is moving velocity of heat source in $x$-direction.

The effect of the moving point heat source on the plate can be the initial condition of the thermal conduction [25]. Therefore, the boundary and initial conditions are expressed as

$$\delta(x).\delta(y) = 0,\ (x \neq vt)\ and\ (y \neq -l) \tag{2}$$

$$T = 0,\ (t = 0) \tag{3}$$

$$T = 0,\ \text{as}\ x^2 + y^2 \to \infty \tag{4}$$

$$\frac{\partial T(x,0^+)}{\partial y} = \frac{\partial T(x,0^-)}{\partial y} = 0,\ (|x| < a) \tag{5}$$

$$T(x,0^+) = T(x,0^-),\ (|x| \geq a) \tag{6}$$

$$\frac{\partial T(x,0^+)}{\partial y} = \frac{\partial T(x,0^-)}{\partial y},\ (|x| \geq a) \tag{7}$$

## 3. Solution of the Temperature Field

The temperature field $T(x, y, t)$ can be expressed as

$$T(x,y,t) = T^1(x,y,t) + T^2(x,y,t) \tag{8}$$

where $T^{(1)}(x, y, t)$ satisfies the following equation and boundary conditions,

$$k\nabla^2 T^{(1)} - \rho c\frac{\partial T^{(1)}}{\partial t} = -q.\delta(x - vt).\delta(y + l) \tag{9}$$

$$\delta(x).\delta(y) = 0,\ (x \neq vt)\ and\ (y \neq -l) \tag{10}$$

$$T^{(1)} = 0,\ (t = 0) \tag{11}$$

$$T^{(1)} = 0,\ \text{as}\ x^2 + y^2 \to \infty \tag{12}$$

Whereas $T^{(2)}(x, y, t)$ is subject to the relations,

$$k\nabla^2 T^{(2)} - \rho c\frac{\partial T^{(2)}}{\partial t} = 0 \tag{13}$$

$$T^{(2)} = 0,\ (t = 0) \tag{14}$$

$$T^{(2)} = 0,\ \text{as}\ x^2 + y^2 \to \infty \tag{15}$$

$$\frac{\partial T^{(2)}(x,0)}{\partial y} = -\frac{\partial T^{(1)}(x,0)}{\partial y}, \ (|x| \le a) \tag{16}$$

$$T^{(2)}(x,0^+) = T^{(2)}(x,0^-) \ (|x| \ge a) \tag{17}$$

$$\frac{\partial T^{(2)}(x,0^+)}{\partial y} = -\frac{\partial T^{(2)}(x,0^-)}{\partial y}, \ (|x| \ge a) \tag{18}$$

### 3.1. Solution of $T^{(1)}(x, y, t)$

Solution of $T^{(1)}(x, y, t)$ is adopted by the moving coordinate method [31-32]. The moving coordinate system $o_1\xi\eta$ is formed by setting the heat source to be the origin of coordinate $o_1$, the $o_1$ is coincidence with the original coordinate system at $t$=0, any point $(x, y)$ in the moving coordinate system is

$$\xi = x - vt, \ \ \eta = y \tag{19}$$

It is obvious that the point heat source is fixed in the moving coordinate system. The temperature field $T'^{(1)} = T'^{(1)}(\xi, \eta, t)$ in the moving coordinate system is

$$T^{(1)} = T^{(1)}\left(x, y, t\right) = T'^{(1)}(\xi + vt, \eta, t) = T'^{(1)}(\xi, \eta, t) \tag{20}$$

Considering $dx=\xi+vdt$ $dy=d\eta$, and

$$\frac{\partial T^{(1)}}{\partial x} = \frac{\partial T'^{(1)}}{\partial \xi} \cdot \frac{\partial T^{(1)}}{\partial y} = \frac{\partial T'^{(1)}}{\partial \eta} \cdot \frac{\partial^2 T^{(1)}}{\partial x^2} = \frac{\partial^2 T'^{(1)}}{\partial \xi^2} \cdot \frac{\partial^2 T^{(1)}}{\partial y^2} = \frac{\partial^2 T'^{(1)}}{\partial \eta^2} \tag{21}$$

$$\frac{\partial T'^{(1)}}{\partial t} = \frac{\partial T^{(1)}}{\partial t} + \frac{\partial T^{(1)}}{\partial x}\frac{dx}{dt} = \frac{\partial T^{(1)}}{\partial t} + \frac{\partial T'^{(1)}}{\partial \xi} \cdot v \tag{22}$$

$$\frac{\partial T^{(1)}}{\partial t} = \frac{\partial T'^{(1)}}{\partial t} - v\frac{\partial T'^{(1)}}{\partial \xi} \tag{23}$$

Eq. (9) can be expressed in the moving coordinate system as following

$$k\nabla_1^2 T'^{(1)} + v\rho c(\frac{\partial T'^{(1)}}{\partial \xi} - \frac{\partial T'^{(1)}}{\partial t}) = -q.\delta(\xi).\delta(\eta + l) \tag{24}$$

where

$$\nabla_1^2 = \frac{\partial^2 T'^{(1)}}{\partial^2 \xi^2} + \frac{\partial^2 T'^{(1)}}{\partial^2 \eta^2} \tag{25}$$

The position of the heat source in the moving coordinate system is fixed, $T'^{(1)}$ has nothing to do with the time $t$. The partial derivative of the formula $T'^{(1)}$ to $t$ does not exist. Let $\lambda = vpc / k$, the heat conduction equation in the moving coordinate system can be simplified by

$$(\nabla_1^2 + \lambda\frac{\partial}{\partial \xi}) \ T'^{(1)}(\xi, \eta) = -\frac{q}{k}.\delta(\xi).\delta(\eta + l) \tag{26}$$

Eq. (26) is a steady expression. Therefore, the boundary and initial conditions in the moving coordinate system are changed into Eqs. (10)-(12) that are expressed by

$$\delta(\xi).\delta(\eta) = 0,\ (\xi \neq 0)\ and\ (\eta \neq -l) \tag{27}$$

$$T'^{(1)} = 0,\ (t = 0) \tag{28}$$

$$T'^{(1)} = 0,\ \text{as}\ \ \xi^2 + \eta^2 \to \infty \tag{29}$$

According to the literature [32-33], the solution of the Eq. (26) under the boundary conditions Eqs. (27)- (29) can be written as

$$T'^{(1)}(\xi,\eta) = \frac{q}{4\pi kr}\ exp\ [-\frac{v}{2k}(\xi + r)] \tag{30}$$

where $r^2 = \xi^2 + \eta^2$

The temperature in original Cartesian coordinate system can be obtained by coordinate transform of Eq. (19).

$$T'^{(1)}(x,y,t) = \frac{q}{4\pi kr}\exp[-\frac{v}{2k}((x - vt) + r)] \tag{31}$$

where $r^2 = (x - vt)^2 + y^2$

*3.2. Solution of $T^{(2)}(x, y, t)$*

According to heat conduction Eq. (13) and the boundary condition of Eqs. (14)-(18), Fourier or Laplace transform is employed to reduce the heat conduction problem to be a singular integral equation that is solved numerically.∫

Application of Laplace transform to Eq. (13) and Eq. (31) leads to the expressions as

$$T^{*(2)}(x,y,p) = \int_0^\infty T^{(2)}(x,y,t)\ exp\ (-pt)dt \tag{32}$$

$$T^{*(1)}(x,y,p) = \int_0^\infty T^{(1)}(x,y,t)\ exp\ (-pt)dt \tag{33}$$

where the superscript "*" denotes the quantities in the Laplace domain and $Br$ represents the Bromwich path of integration.

Application of Laplace transforms to Eq. (13) and Eqs. (14)- (18) leads to the expressions as

$$k\nabla^2 T^{*(2)}(x,y,p) = \rho cpT^{*(2)}(x,y,p) \tag{34}$$

$$T^{*(2)} = 0,\ (t = 0) \tag{35}$$

$$T^{*(2)} = 0,\ \text{as}\ \ x^2 + y^2 \to \infty \tag{36}$$

$$\frac{\partial T^{*(2)}(x,0)}{\partial y} = -\frac{\partial T^{*(1)}(x,0)}{\partial y},\ (|x| \le a) \tag{37}$$

$$T^{*(2)}(x,0^+) = T^{*(2)}(x,0^-)\ (|x| \ge a) \tag{38}$$

$$\frac{\partial T^{*(2)}(x,0^+)}{\partial y} = -\frac{\partial T^{*(2)}(x,0^-)}{\partial y}\ (|x| \ge a) \tag{39}$$

Applying the Fourier transform to Eq. (34), the $T^{*(2)}(x,y,p)$ satisfying the boundary condition Eqs. (35)-(39) can be expressed as

$$T^{*(2)}(x,y,p) = \int_{-\infty}^{\infty} E(w)\ exp\ (-gy)\ exp\ (-ixw)dw\ \ y \ge 0 \tag{40}$$

$$T^{*(2)}(x,y,p) = \int_{-\infty}^{\infty} \frac{E(w)}{1 + \exp(2gl)}[exp(-gy) - exp(2gl + gy)]exp(-ixw)dw\ \ y \le 0 \tag{41}$$

where $E(w)$ are unknown functions to be determined.

$$g = \sqrt{w^2 + \lambda p} \tag{42}$$

$$\lambda = pc / k \tag{43}$$

The density function is introduced as

$$\vartheta(x) = \frac{\partial T^*(x,0^+)}{\partial x} - \frac{\partial T^*(x,0^-)}{\partial x} \tag{44}$$

where $T^*(x, y, p) = T^{*(1)}(x, y, p) + T^{*(2)}(x, y, p)$.

It is clear from the boundary condition Eq. (37) that the expression can be obtained as

$$\begin{cases} \int_{-a}^{a} \vartheta(x)dx = 0 \\ \vartheta(x) = 0 \quad (|x| \geq a) \end{cases} \tag{45}$$

Substituting Eqs. (40)- (41) into Eq. (45), the unknown function $E(w)$ can be expressed as

$$E(w) = \frac{i[1 + exp(2gl)]}{4\pi w \, exp(2gl)} \int_{-1}^{1} \vartheta(t) \, exp(itw)dt \tag{46}$$

Substituting Eq. (40), Eq. (41) and Eq. (33) into Eq. (37), the singular integral equation for can be obtained by applying Eq. (46) as following

$$\int_{-1}^{1} \vartheta(t)[\frac{1}{t-x} + k'(x,t)]dt = -2\pi \frac{\partial T^{*(1)}(X,0)}{\partial y} \tag{47}$$

where the kernel function $k'(x,t)$ is expressed as following

$$k'(x,t) = \int_0^{\infty} \{1 - \frac{g}{w}[1 + exp(-2gl)]\} \sin[w(x-t)]dw \tag{48}$$

The integral Eq. (47) under the singled-value condition in Eq. (45) has the following form of solution [27-28]:

$$\vartheta(x) = \frac{\theta(x)}{\sqrt{1-x^2}}, \quad |x| < a \tag{49}$$

where $\theta(x)$ is bounded and continuous on the interval [-$a$, $a$]. Function $\theta(x)$ can be solved numerically, which has been addressed in Chen and Hu [27-28]. $E(w)$ is calculated by the Chebyshev quadrature for integration as

$$E(w) \cong \frac{1 + exp(-2gl)}{4\pi w} \sum_{m=1}^{n} \omega_m \theta(\xi_m) \sin(w\xi_i) \tag{50}$$

$$\xi_i = \cos(\frac{2m-1}{2n}\pi) \, . \, m = 1, 2 \ldots\ldots n \tag{51}$$

$$\omega_m = \frac{\pi}{n} \tag{52}$$

The substitution of Eq. (50) into Eqs. (40)-(41) can give the $T^{*(2)}(x, y, p)$ in $p$-plane, the $T^{*(2)}(x, y, t)$ in time domain can be given by applying the Laplace inverse transform, then the $T(x, y, t)$ in time domain can be given by Eq. (31) and Eq. (8).

## 4. Numerical results and discussions

The parameters used in the numerical computation are the heat intensity $p$=1 and $l$= -1. The distribution of temperature field of the body without crack is shown in Fig. 2. The distributions of temperature field of the cracked body are shown in Figs. 3-5.

Fig. 2 displays the temperature of the body without crack subjected to the moving point source for the cases of $v$=1.0, $l$=-1 and $t$=0.5, $v$=1.0, $l$=-1 and $t$=1, $v$=1.0, $l$=-1 and $t$=1.5, $v$=2.0, $l$=-1 and $t$=0.5 respectively. The temperature decreases as the distance increases from the point heat source, there is no thermal disturbance in the body. In Fig. 2(b) and Fig. 2(c), under the unchanged condition of the moving speed $v$, it is clear that the highest temperature of the Fig. 2(b) is kept in constant with that of the Fig. 2(c) with the same isotherms range. In Figs. 2(a), (b), and 2(d), under the increasing condition of the moving speed $v$ of the point heat source, the highest temperatures decrease as well as the isotherms range. The temperature distribution o f the body without crack subjected to the transient point source in Fig. 2 is consistent with the ones of the existing literatures of the Ref. [1] and Ref. [13].

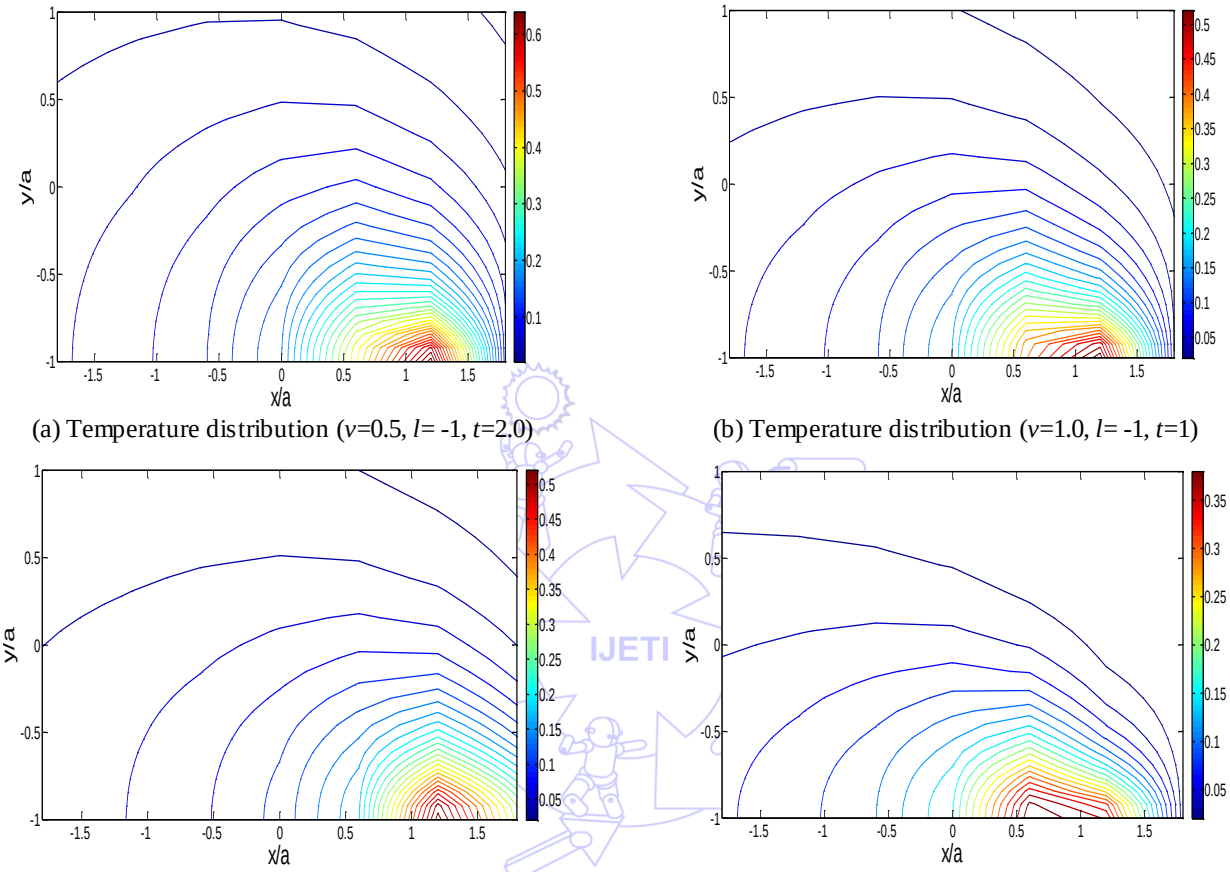


(a) Temperature distribution ($v$=0.5, $l$= -1, $t$=2.0)

(b) Temperature distribution ($v$=1.0, $l$= -1, $t$=1)

(c) Temperature distribution ($v$=1.0, $l$= -1, $t$=1.5)

(d) Temperature distribution ($v$=2.0, $l$= -1, $t$=0.5)

Fig. 2 The distribution of temperature field in the body without crack

The disturbance of the thermally insulated crack on the temperature field can be observed from the temperature contours lines in Figs. 3-4, and there is a temperature jump across the crack faces. In Figs. 3-5, it can be seen that the temperature distribution in the cracked layers varies as the speed and the times of the moving point heat source. The interference of the insulated crack also results in different temperature distribution to that of Fig. 2.

The temperature distribution in the cracked body varies as the moving speed v of the point heat source changes, which is shown in Fig. 3. Under the unchanged condition of the positions of the point heat source, the highest temperatures and the isotherms range decrease in the increasing condition of the moving speed v of the point heat source.

At the same moving speed $v$ of the point heat source, the temperature distribution in the cracked body varies as the time changes, which is shown in Fig. 4. Under the unchanged condition of the moving speed $v$ of the point heat source, the highest temperatures and the isotherms range being closer to crack face are both higher than that of the further one because of the interference of the insulated crack.

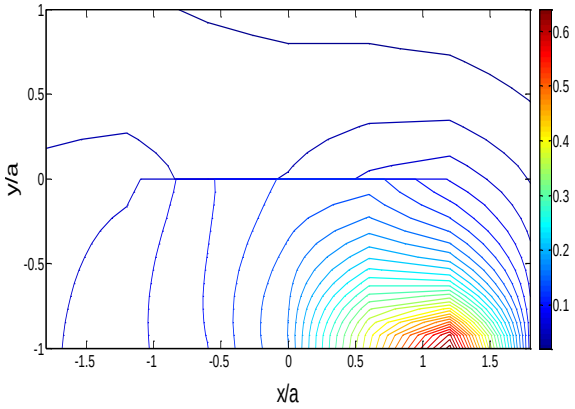


(a) Temperature distribution in cracked plate (v=0.5, l= -1, t=2.0)

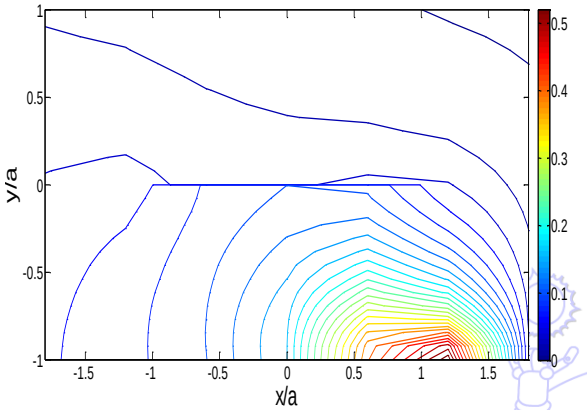


(b) Temperature distribution in cracked layers ($v$=1.0, $l$= -1, $t$=1.0)

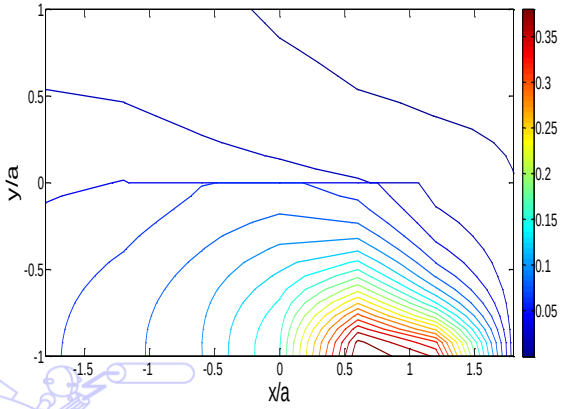


(c) Temperature distribution in cracked layers ($v$=2.0, $l$= -1, $t$=0.5)

Fig. 3 Temperature distribution in cracked layers at different speeds

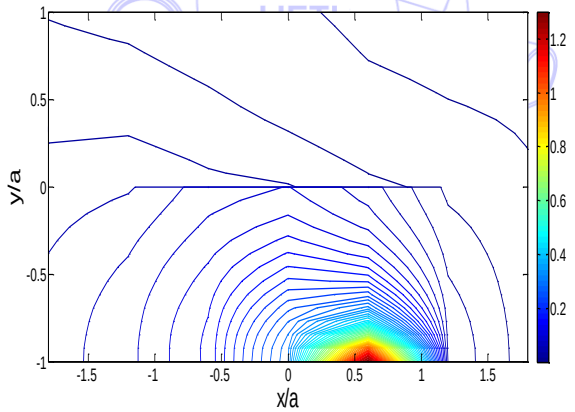


(a) Temperature distribution in cracked plate ($v$=1.0, $l$= -1 , $t$=0.5)

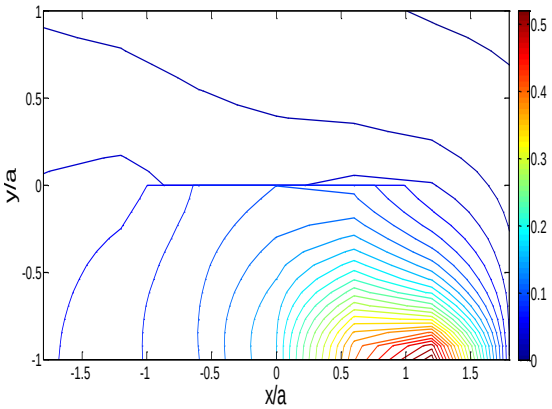


(b) Temperature distribution in cracked layers ($v$=1.0, $l$= -1, $t$=1.0)

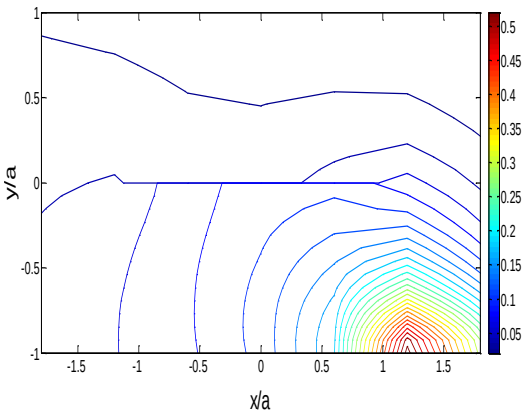


(c) Temperature distribution in cracked layers ($v$=1.0, $l$= -1, $t$=1.5)

Fig. 4 Temperature distribution in cracked layers at different positions of the point source

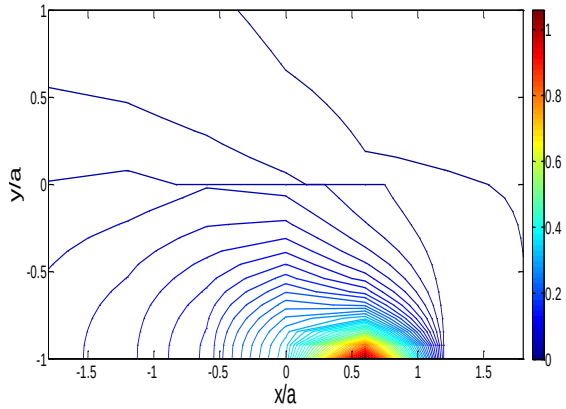


(a) Temperature distribution in cracked plate ($v$=2.0, $l$= -1, $t$=0.25)

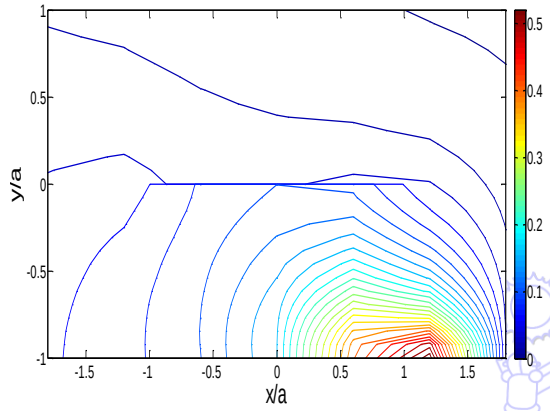


(b) Temperature distribution in cracked layers ($v$=1.0, $l$= -1, $t$=1.0)

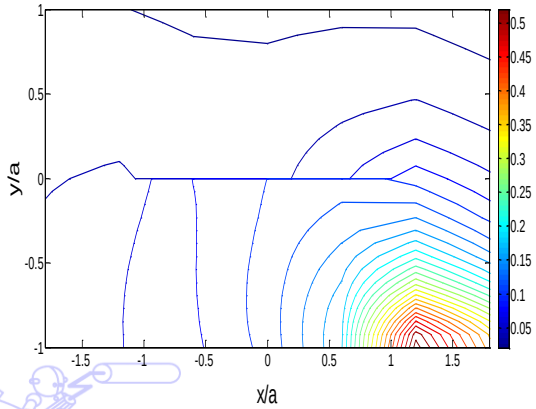


(c) Temperature distribution in cracked layers ($v$=0.5, $l$= -1 and $t$=2.5)

Fig. 5 Temperature distribution in cracked layers at different speeds and times

The temperature distribution in the cracked body varies as the moving speed v of the point heat source and time change, which is shown in Fig. 5. It is interesting that the highest temperatures and the isotherms range of the case of the higher moving speed $v$ are both higher than that of the lower moving speed $v$ due to the interference of the insulated crack. The interference of the insulated crack results in different temperature distribution to that of Fig. 2.

The temperature distribution on the crack faces interrupted by the insulated crack is much more attracted. For the cases of $v$=0.5, $l$=-1 and $t$=2.0, $v$=1.0, $l$=-1 and $t$=1.0, $v$=2.0, $l$=-1 and $t$=0.5, the temperature on the crack faces and extension line are displayed in Fig. 6. For the cases of $v$=1.0, $l$=-1 and $t$=0.5, $v$=1.0, $l$=-1 and $t$=1.0, $v$=1.0, $l$=-1 and $t$=1.5, the temperature on the crack faces and extension line are displayed in Fig. 7. The temperature distribution is disturbed by the insulated crack. There is a temperature jump across crack face, the temperature on the crack extension line is continuous. The temperatures on crack face and the extended line both vary as the time and the location of the point source change.

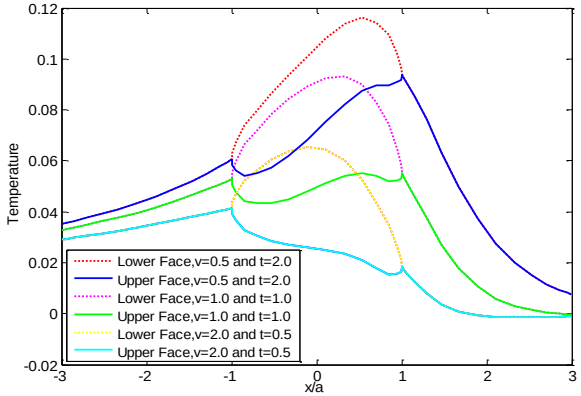


Fig. 6 Temperature distribution on crack faces and extended lines ($v$=0.5, $l$= -1, $t$=2.0, $v$=1.0, $l$= -1, $t$=1.0, $v$=2.0, $l$= -1, $t$=0.5)

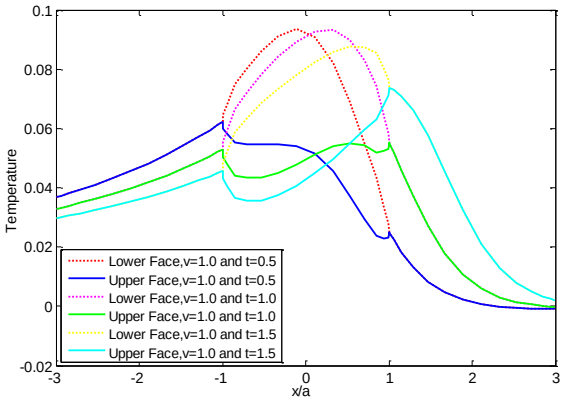


Fig. 7 Temperature distribution on crack faces and extended lines ($v$=1.0, $l$= -1, $t$=0.5, $t$=1.0, $t$=1.5)

## 5. Conclusions

The temperature distribution of a cracked half-plane under moving point heat source has been computed and analyzed by the analytical solution and the numerical means. The numerical examples of the temperature distribution under moving point heat source are investigated and discussed. Numerical studies show that the interference of the insulated crack results in different temperature distribution to that of non-crack plate structure. The temperature distribution in the cracked layers varies as the speed and the effect time of the moving point heat source.

For cases of the temperature distribution of the body without crack, the temperature decreases as the distance increases from the point heat source, there is no thermal disturbance in the body. Under an increasing of the moving speed of the point heat source, the highest temperatures decrease as well as the isotherms range. For cases of the disturbance of the thermally insulated crack to the temperature field, there is a temperature jump across the crack faces. The temperature distribution in the cracked layers varies as the speed and the effect time of the moving point heat source. Under the unchanged condition of the moving speed of the point heat source, the highest temperature and isotherm range of the case being closer to crack face are higher than that of the further one. The highest temperature and the isotherm range of the case of the higher moving speed are greater than that of the lower moving speed due to the interference of the insulated crack.

## Acknowledgements

This supports, by National Natural Science Foundation of China (51475159, 51405156) and Hunan Provincial Natural Science Foundation of China (2017JJ1015, 2017JJ2086), are gratefully acknowledged.

## References

[1] X. K. Zhu and Y. J. Chao, "Numerical simulation of transient temperature and residual stresses in friction stir welding of 304L stainless steel," Journal of Materials Processing Technology, vol. 146, no. 2, pp. 263-272, 2004.
[2] T. Boellinghaus, Hot cracking phenomena in welds, Berlin: Springer, pp. 3-18, 2005.
[3] D. Rosenthal, "The theory of moving sources of heat and its application to metal treatments," Transactions of The ASME, vol. 68, no. 8, pp. 849-866, 1946.
[4] K. Masubuchi and D. W. Hopkins, Analysis of welded structures, 1st ed. London: Pergamon Press, 1980.
[5] G. M. Oreper and J. Szekely, "Heat and fluid-flow phenomena in weld pools," Journal of Fluid Mechanics, vol. 147, pp. 53-79, 1984.
[6] R. T. C. Choo, J. Szekely, and R. C. Westhoff, "On the calculation of the free surface temperature of gas-tungsten-arc weld pools from first principles: part I. modeling the welding arc," Metallurgical Transactions, vol. 23, no. 3, pp. 357-369, 1992.
[7] J. J. Lowke, R. Morrow, and J. Haidar, "A simplified unified theory of arcs and their electrodes," Journal of Physics D Applied Physics, vol. 30, no. 14, pp. 2033-2042, 1997.
[8] S. Kou and Y. H. Wang, "Computer simulation of convection in moving arc weld pools," Metallurgical and Materials Transactions A, vol. 17, no. 12, pp. 2271-2277, 1986.

[9] S. D. Kimand S. J. Na, "A study on heat and mass flow in stationary gas tungsten arc welding using the numerical mapping method," Proc. of the Institution of Mechanical Engineers Part B Journal of Engineering Manufacture, 1989, pp. 233-242.
[10] H. G. Fan and Y. W. Shi, "Numerical simulation of the arc pressure in gas tungsten arc welding," Journal of Materials Processing Technology, vol. 61, pp. 302-308, 1996.
[11] Y. Joshi, P. Dutta, P. E. Schupp, and D. Espinosa, "Nonaxisymmetric convection in stationary gas tungsten arc weld pools," Journal of Heat Transfer, vol. 119, no. 1, pp. 164-172, 1997.
[12] M. Tanaka, H. Terasaki, M. Ushio, and J. J. Lowke, "A unified numerical modeling of stationary tungsten-inert-gas welding process," Metallurgical and Materials Transactions A, vol. 33, no. 7, pp. 2043-2052, 2002.
[13] Y. H. Wei, Z. B. Dong, R. P. Liu, and Z. J. Dong, "Three-dimensional numerical simulation of weld solidification cracking," Modelling & Simulation in Materials Science & Engineering, vol. 13, no. 3, pp. 437-454, 2005.
[14] J. Hu and H. L. Tsai, "Heat and mass transfer in gas metal arc welding, part I: the arc," International Journal of Heat and Mass Transfer, vol. 50, pp. 833-846, 2007.
[15] A. H. Yaghi, T. H. Hyde, A. A. Becker, and W. Sun, "Finite element simulation of welding and residual stresses in a P91 steel pipe incorporating solid-state phase transformation and post-weld heat treatment," The Journal of Strain Analysis for Engineering Design, vol. 43, no. 5, pp. 275-293, 2008.
[16] R. Das, K. S. Bhattacharjee, and S. Rao, "Welding heat transfer analysis using element free galerkin method," Advanced Materials Research, vol. 410, pp. 298-301, 2011.
[17] M. Sheikhi, F. M. Ghaini, and H. Assadi, "Solidification crack initiation and propagation in pulsed laser welding of wrought heat treatable aluminum alloy," Science and Technology of Welding and Joining, vol. 19, no. 3, pp. 250-255, 2014.
[18] G. C. Sih, "Heat conduction in the infinite medium with lines of discontinuities," Journal of Heat Transfer, vol. 87, no. 2, pp. 283-298, 1965.
[19] Y. T. Da, "Characteristics of thermal and flow behavior in the vicinity of discontinuities," International Journal of Heat and Mass Transfer, vol. 35, no. 2, pp. 481-491, 1992.
[20] N. Noda and Z. H. Jin, "Thermal stress intensity factors for a crack in a strip of a functionally gradient material," International Journal of Solids and Structures, vol. 30, no. 8, pp. 1039-1056, 1993.
[21] Y. Zhou, X. Li, and D. Yu, "A partially insulated interface crack between a graded orthotropic coating and a homogeneous orthotropic substrate under thermal flux supply," International Journal of Solids & Structures, vol. 47, no. 6, pp. 768-778, 2010.
[22] Z. H. Jin and N. Naotake, "Transient thermal stress intensity factors for a crack in a semi-infinite plate of a functionally gradient material," International Journal of Solids and Structures, vol. 31, no. 2, pp. 203-218, 1994.
[23] J. J. Mason and A. J. Rosakis, "On the dependence of the dynamic crack tip temperature fields in metals upon crack tip velocity and material parameters," NASA Sti/recon Technical Report N, vol. 93, pp. 337-350, 1992.
[24] C. Y. Chang and C. C. Ma, "Transient thermal conduction of a rectangular plate with multiple insulated cracks by the alternating method," International Journal of Heat & Mass Transfer, vol. 44, pp. 2423-2437, 2001.
[25] A. Zamani, R. B. Hetnarski, and M. R. Eslami, "Second sound in a cracked layer based on Lord-Shulman theory," Journal of Thermal Stresses, vol. 34, no. 3, pp. 181-200, 2011.
[26] B. L. Wang and J. C. Han, "A crack in a finite mediumunder transient non-Fourier heat conduction," International Journal of Heat & Mass Transfer, vol. 55, no. 17, pp. 4631-4637, 2012.
[27] Z. T. Chen and K. Q. Hu, "Thermo-elastic analysis of a cracked half-plane under a thermal shock impact using the hyperbolic heat conduction theory," Journal of Thermal Stresses, vol. 35, no. 4, pp. 342-362, 2012.
[28] K. Q. Hu and Z. T. Chen, "Transient heat conduction analysis of a cracked half-plane using dual-phase-lag theory," International Journal of Heat and Mass Transfer, vol. 62, no. 1, pp. 445-451, 2013.
[29] M. Turkyilmazoglu, "Heat transfer from warm water to a moving foot in a footbath," Applied Thermal Engineering, vol. 98, pp. 280-287, 2016.
[30] M. Turkyilmazoglu, "Anomalous heat transfer enhancement by slip due to nanofluids in circular concentric pipes," International Journal of Heat and Mass Transfer, vol. 85, pp. 609-614, 2015.
[31] P. P. Teodorescu, Introduction to thermoelasticity, Beijin: Tsinghua University Press, 1989.
[32] H. S. Carslaw and J. C. Jaeger, Conduction of heat in solids, Oxford University Press, 2 ed., 1986.
[33] Y. Tanigawa, S. Kuriyama, and Y. Takeuti, "Transient thermal stress analysis of a strip with finite width under consideration of the heated boundary moving with constant velocity," Transactions of the Japan Society of Mechanical Engineers Series A, vol. 51, no. 464, pp. 1042-1049, 1985.